# Genetics, Clinical Characteristics, and Natural History of *PDE6B*-Associated Retinal Dystrophy

SHAIMA AWADH HASHEM, MICHALIS GEORGIOU, YU FUJINAMI-YOKOKAWA, YANNIK LAICH, MALENA DAICH VARELA, THALES A.C. DE GUIMARAES, NASER ALI, OMAR A. MAHROO, ANDREW R. WEBSTER, KAORU FUJINAMI, AND MICHEL MICHAELIDES

- PURPOSE: To analyze the clinical characteristics, natural history, and genetics of *PDE6B*-associated retinal dystrophy.
- DESIGN: Retrospective, observational cohort study.
- METHODS: Review of medical records and retinal imaging, including fundus autofluorescence (FAF) imaging and spectral-domain optical coherence tomography (SD-OCT) of patients with molecularly confirmed *PDE6B*-associated retinal dystrophy in a single tertiary referral center. Genetic results were reviewed, and the detected variants were assessed.
- RESULTS: Forty patients (80 eyes) were identified and evaluated longitudinally. The mean age (±SD, range) was 42.1 years (± 19.0, 10-86) at baseline, with a mean follow-up time of 5.2 years. Twenty-nine (72.5%) and 27 (67.5%) patients had no or mild visual acuity impairment at baseline and last visit, respectively. Best-corrected visual acuity (BCVA) was 0.56 ± 0.72 LogMAR (range −0.12 to 2.80) at baseline and 0.63 ± 0.73 LogMAR (range 0.0-2.80) at the last visit. BCVA was symmetrical in 87.5% of patients. A hyperautofluorescent ring was observed on FAF in 48 and 46 eyes at baseline and follow-up visit, respectively, with a mean area of 7.11 ± 4.13 mm$^2$ at baseline and mean of 6.13 ± 3.62 mm$^2$ at the follow-up visit. Mean horizontal ellipsoid zone width at baseline was 1946.1 ± 917.2 µm, which decreased to 1763.9 ± 827.9 µm at follow-up. Forty-four eyes had cystoid macular edema at baseline (55%), and 41 eyes (51.3%) at follow-up. There were statistically significant changes during the follow-up period in terms of BCVA and the ellipsoid zone width. Genetic analysis identified 43 variants in the *PDE6B* gene, including 16 novel variants.
- CONCLUSIONS: This study details the natural history of *PDE6B*-retinopathy in the largest cohort to date. Most patients had mild to no BCVA loss, with slowly progressive disease, based on FAF and OCT metrics. There is a high degree of disease symmetry and a wide window for intervention. (Am J Ophthalmol 2024;263: 1–10. © 2024 The Author(s). Published by Elsevier Inc. This is an open access article under the CC BY license (http://creativecommons.org/licenses/by/4.0/))

RETINITIS PIGMENTOSA (RP) (OMIM #268000) IS THE most common hereditary retinal disease. It is characterized by progressive retinal degeneration that causes symptoms of early nyctalopia and peripheral field constriction, eventually affecting the central vision and leading to legal blindness.[1] One in 3 to 4000 in the population has RP, and it can be inherited as autosomal recessive in 50% to 60% of cases, 30% to 40% as autosomal dominant and the remaining ∼5% to 15% as X-linked inheritance.[2,3] Nonsyndromic RP has been associated with more than 80 genes, more than 35 which have been associated with an autosomal recessive mode of inheritance.[4]

Phosphodiesterase 6 (PDE6) enzyme is a heterotetrameric protein that consists of alpha (PDE6A), beta (PDE6B), and 2 gamma subunits (PDE6G).[5] Up to 8% of patients with autosomal recessive RP have variants in the *PDE6B* gene (RP6).[6] *PDE6B* is located on chromosome 4p16.3 (OMIM *180072) and has 22 coding exons that encodes 854 amino acid residues.[5] Disease-causing sequence variants in the *PDE6B* homolog (RefSeq accession number, NM_000283.3) have also been reported to cause rod and cone degeneration in animal models.[7] In rod and cone photoreceptors, PDE6 is the primary regulator of cytoplasmic

cGMP concentration which is essential for the phototransduction cascade. Retinal degeneration and photoreceptor cell death is caused when disruption of the visual signaling pathway is caused by the continuous imbalance in cGMP metabolism (either in its synthesis or degradation).[8]

PDE6B-associated RP has no cure currently, though different treatments are under investigation. Partial improvements in visual function and pupil reflex were documented when chemically induced photoreceptor-like cells (CiPCs) were transplanted into the subretinal space of rd1 mice, which are a homozygous mutant for PDE6B.[9] Also, subretinal gene therapy during postnatal development of the retina showed positive visual effects in PDE6B-deficient mice and dogs.[10-12] Gene therapy treatment in humans is currently under investigation in patients with biallelic variants in PDE6B (NCT03328130) and (NCT05748873).[13] Despite the on-going therapeutics efforts, data on the natural history of the disease are limited.

In this study, we aim to provide a detailed report of the clinical and molecular genetic findings, investigate genotype-phenotype correlations and describe the disease natural history by analyzing a large cohort with PDE6B-associated retinopathy. This will enhance counseling, prognostication, and trial design.

## METHODS

The study adhered to the tenets of the Declaration of Helsinki and was approved by the local ethics committee.

- PATIENTS: Patients with molecularly confirmed PDE6B-associated retinopathy were identified by reviewing the clinical records and genetics database of Moorfields Eye Hospital (London, UK). All patients harbor 2 or more PDE6B variants, and were seen by retina genetics specialists (MM, OM, ARW). Patients with other pathologies or questionable diagnosis were excluded from further analysis.

- CLINICAL DATA: Review of clinical records, including medical and ocular histories, slit-lamp biomicroscopy, and a dilated funduscopic examination was performed. Age of onset was defined as the age of the first reported symptoms. The best-corrected visual acuity (BCVA) was measured using Snellen charts and converted into logarithm of the minimum angle of resolution (LogMAR) units. LogMAR BCVA was employed as a surrogate for central vision function. BCVA was used to categorize eyes into 1 of 4 groups based on the World Health Organization visual impairment criteria: (1) no or mild impairment, as visual acuity <0.48 LogMAR; (2) moderate impairment, as 0.48 to 1 LogMAR; (3) severe impairment 1 to 1.3 LogMAR; and (4) blindness, as greater than 1.3 LogMAR.[14,15] Interocular symmetry was defined as a difference ≤0.3 LogMAR

(equivalent to 15 Early Treatment of Diabetic Retinopathy Study (ETDRS) letters) between eyes.

Refraction was undertaken by an optometrist for both adults and children, and spherical equivalent was calculated for refractive error. Visual field testing, if available, was performed with either confrontational visual field testing, kinetic perimetry using Goldmann perimeter and static perimetry using 2 devices (Humphrey 750i Visual Field Analyzer, Humphrey Instruments; Octopus 900, Haag Streit). Each patient's clinical assessment was reviewed and analyzed at 2 points in time with an interval period from baseline that ranged between 3 months and 12 years.

- RETINAL IMAGING: Color fundus photography (Optos ultra widefield camera, Optos; or Topcon), infrared reflectance (IR), spectral domain optical coherence tomography (SD-OCT, Spectralis OCT, Heidelberg Engineering) and short-wavelength (488-nm) fundus autofluorescence (FAF) imaging were performed longitudinally for most patients. Analysis was performed using all available data.

The area of the hyperautofluorescent ring at the macula was quantified by the manufacturer software (Heyex version 1.9.14.0; Heidelberg Engineering) or adjusted manually as needed by a trained ophthalmologist (SH). Foveal central macular volume scans in SD-OCT images were performed in a 6 × 6 mm square that included the standard 1-, 3-, and 6-mm grid template from the ETDRS grid. Inner limiting membrane and Bruch membrane were automatically segmented and the width of preserved photoreceptor ellipsoid zone (EZW) line at the macula was measured by the manufacturer software (Heyex version 1.9.14.0; Heidelberg Engineering) or adjusted manually as needed by a trained ophthalmologist (SH). Each patient's clinical images were reviewed and analyzed at two points of time; presentation (baseline) and last follow-up.

- LONGITUDINAL ASSESSMENT OF VISUAL ACUITY AND IMAGING PARAMETERS: The following clinical parameters were longitudinally assessed: BCVA, the presence of the hyperautofluorescent ring, the area of the hyperautofluorescent ring, macular thickness, macular volume, the presence of preserved EZ line, the EZW, and the presence of cystoid macular edema (CMO). Comparison analyses between baseline and follow-up visit were performed for the aforementioned clinical parameters.

- MOLECULAR GENETICS: A combination of Sanger direct sequencing and next-generation sequencing, including panel testing of retinal dystrophy genes, whole exome sequencing, and whole genome sequencing, was used to identify variants in the PDE6B gene. All recruited patients were reassessed for their detected PDE6B variants. All detected PDE6B variants were analyzed comprehensively. Sequence variant nomenclature was obtained according to the guidelines of the Human Genome Variation Society by using Mutalyzer 2.0. (Refseq Reference: NM_000283.3; En-

semble transcript ID: ENST00000496514.6; UniProtKB: P35913).[16] Pathogenicity assessment of all detected variants was performed based on the guidelines of the American College of Medical Genetics and Genomics.[17,18] *In silico* molecular modeling is described in Supplementary Methods.

• GENOTYPE-PHENOTYPE ANALYSES: Patients were classified into 3 genotype groups based on the presence of null variants: genotype A (multiple null variants), genotype B (one null and one non-null variants), and genotype C (multiple non-null variants). Clinical parameters were compared between each of the genotype groups cross-sectionally.

• STATISTICAL ANALYSIS: Data were analyzed using IBM SPSS software package version 20.0. (IBM Corp). Categorical data were represented as numbers and percentages. The marginal homogeneity test was used for categorical variables to analyze the significance between 2 visits. For continuous numerical data, normality was tested using the Kolmogorov-Smirnov test. Quantitative data were expressed as range (minimum and maximum), mean, standard deviation, median, and interquartile range for normally distributed quantitative variables. F-test (ANOVA) was applied for normally distributed quantitative variables to compare between more than 2 groups, and the post hoc test (Tukey) for pairwise comparisons. The paired *t*-test was employed for normally distributed quantitative variables, to compare between baseline and follow-up. The Mann-Whitney test was utilized for non-normally distributed quantitative variables, to compare 2 studied groups, while Kruskal-Wallis test was used for non-normally distributed quantitative variables, to compare between more than 2 studied groups, and post hoc (Dunn's multiple comparisons test) for pairwise comparisons. Non-normally distributed quantitative variables were evaluated with Wilcoxon signed ranks test between 2 visits. Significance of the obtained results was determined at the 5% level.

# RESULTS

• CLINICAL PRESENTATION: Eighty eyes of 40 patients with a clinical diagnosis of RP were included in the study. The cohort consisted of 13 males and 27 females. The mean age at baseline was 42.1 years (±19.0, range 10-86 years), with an average follow-up time of 5.2 years (±3.4, range 0.25-12 years). The mean age of diagnosis was 17.9 years (±11.9, n = 30, range 4.0-55.0 years), while the mean age of symptom onset was 6.9 years (±3.2, n = 25, range 2.0-14.0 years). Thirty-eight patients experienced their first symptoms in childhood, with 18 presenting in the first decade of life, 7 in the second decade, and 13 in childhood without

**TABLE 1.** Demographics and Presenting Symptoms

| | |
|---|---|
| Age (years) (*n* = 40) | |
| Min.-Max. | 10.0-86.0 |
| Mean ± SD. | 42.1 ± 19.0 |
| Median (IQR) | 42.0 (27.0-57.0) |
| **Gender (*n* = 40)** | |
| Male | 13 (32.5%) |
| Female | 27 (67.5%) |
| **Follow up interval, years (*n* = 38)** | |
| Min.-Max. | 0.25-12.0 |
| Mean ± SD. | 5.22 ± 3.47 |
| Median (IQR) | 4.0 (2.0-7.0) |
| **Age of onset (*n* = 25)** | |
| Min.-Max. | 2.0-14.0 |
| Mean ± SD. | 6.96 ± 3.28 |
| Median (IQR) | 6.0 (5.0-10.0) |
| **Age at diagnosis (*n* = 30)** | |
| Min.-Max. | 4.0-55.0 |
| Mean ± SD. | 17.9 ± 11.91 |
| Median (IQR) | 14.0 (10.0-22.0) |
| **Presenting symptoms (*n* = 40)** | |
| No symptoms | 1 (2.5%) |
| Nyctalopia | 27 (67.5%) |
| Nyctalopia and VF constriction | 11 (27.5%) |
| VA reduction | 1 (2.5%) |

*n* = patients; VA = visual acuity; VF = visual field.

specific age documentation. Two patients had no recorded age of onset.

The most common initial symptom was nyctalopia, observed in 27 out of 40 patients (67.5%), while 11 out of 40 (27.5%) presented with both nyctalopia and visual field constriction. Reduced visual acuity was the presenting symptom for 1 patient, and 1 patient was asymptomatic at diagnosis, identified through the diagnosis of a symptomatic sibling. Demographic and presenting symptoms are summarized in Table 1, and symptoms and their age of manifestation are listed in Table 2.

• VISUAL ACUITY: Table 3 summarizes the longitudinal assessment of BCVA. At baseline, the mean BCVA was 0.56 ± 0.72 LogMAR (range: −0.12 to 2.80 LogMAR), while at follow-up, it was 0.63 ± 0.73 LogMAR (range: 0.0-2.80 LogMAR). The mean age (±SD) at baseline was 17.0 ± 11.6 years, with an annual rate of loss of 0.05 LogMAR per year. Follow-up periods ranged from 0.25 to 12 years, with a mean of 5.2 ± 3.4 years. Figure 1, A presents the BCVA against age at baseline for the cohort.

At baseline, 14 out of 80 eyes (17.5%) had no visual acuity impairment. Visual impairment was mild in 56.2% (45/80) of eyes, moderate in 10% (8/80), and severe in 5% (4/80). Nine eyes (11.2%) were blind. At the last follow-up, 9 out of 80 eyes (11.2%) had no visual acuity impairment, 45 (56.2%) were mild, 7 (8.7%) were moderate, 6 (7.5%)
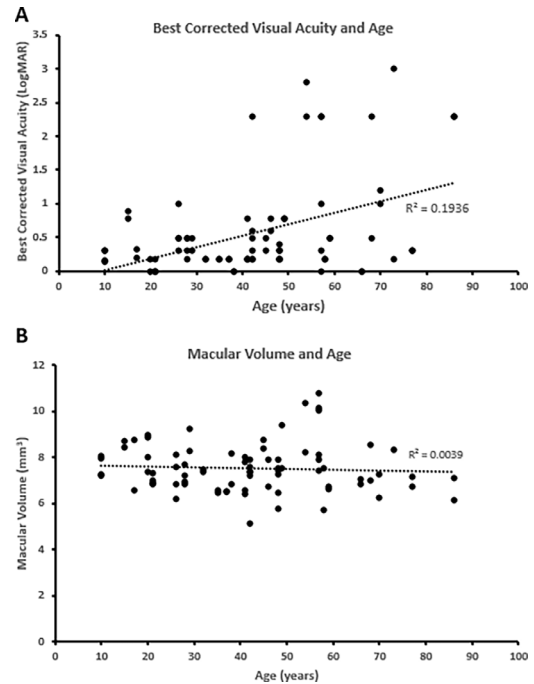
**TABLE 2.** Symptoms and Presenting Age

| | |
|---|---|
| **Reduced VA (*n* = 40)** | |
| No | 20 (50%) |
| **Yes** | **20 (50%)** |
| **At age (y) (*n* = 20)** | |
| Min.-Max. | 3.0-50.0 |
| Mean ± SD. | 17.05 ± 11.67 |
| Median (IQR) | 13.0 (8.0-22.5) |
| **Nystagmus (*n* = 40)** | |
| No | 40 (100%) |
| **Yes** | **0 (0%)** |
| **Nyctalopia (*n* = 40)** | |
| No | 3 (7.5%) |
| Yes | 37 (92.5%) |
| **At age (y) (*n* = 21)** | |
| Min.-Max. | 2.0-14.0 |
| Mean ± SD. | 6.76 ± 3.37 |
| Median (IQR) | 6.0 (5.0-10.0) |
| **Photophobia (*n* = 40)** | |
| No | 37 (92.5%) |
| **Yes** | **3 (7.5%)** |
| **At age (y) (*n* = 3)** | |
| Min.-Max. | 4.0-40.0 |
| Mean | 18.33 |
| Median (IQR) | 11.0 (7.5-25.5) |
| **VF constriction (*n* = 40)** | |
| No | 27 (67.5%) |
| **Yes** | **13 (32.5%)** |
| **At age (y) (*n* = 13)** | |
| Min.-Max. | 3.0-32.0 |
| Mean ± SD. | 10.77 ± 7.89 |
| Median (IQR) | 8.0 (6.0-14.0) |

IQR = interquartile range; VA = visual acuity; VF = visual field; y = years. The percentages in bold describes the distribution of the sample in terms of demographics and symptoms, this is further described in the discussion part.



FIGURE 1. Scatter plots. (A) Scatter plot of the best corrected visual acuity (BCVA) in LogMAR units against age at baseline evaluation for the cohort, with slow deterioration over decades. (B) Scatter plot of the foveal central macular volume against age, with stability over time.
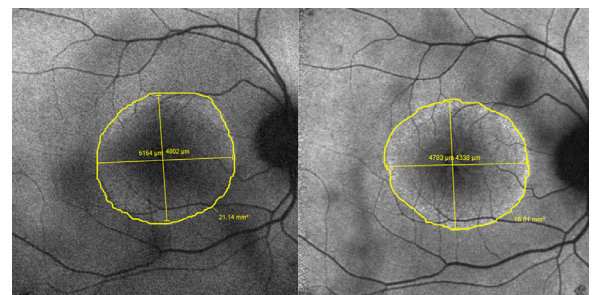


FIGURE 2. Fundus autofluorescence imaging of a patient with *PDE6B*-associated retinitis pigmentosa (RP). At baseline visit (right), a hyperautofluorescent ring commonly observed in RP patients is identified and measured. At follow-up, 2 years later, constriction of the hyperautofluorescent ring was observed.

were severe, 9 (11.2%) were blind, and 4 eyes had no further recorded visual acuity due to no further visits following baseline evaluation. Longitudinal changes in BCVA were statistically significant (*P* = .021; Table 3).

• FAF ANALYSIS: FAF images were available for 92% of eyes. A common finding, a parafoveal hyperautofluorescent ring, was observed. However, in 9/80 (11.3%) at baseline and 10/80 (12.5%) at last follow-up visit, the ring could not be documented due to image quality, lack of recorded images, or no further visits. A hyperautofluorescent ring was identified in 48 out of 71 eyes (67.6%) at baseline and in 46 out of 70 eyes (65.7%) at follow-up. The area within this ring reduced in all eyes. At baseline, the ring area ranged from 1.59 to 21.14 mm$^2$, while at follow-up, it ranged from 1.38 to 16.55 mm$^2$. The mean annual rate of reduction was 0.31 mm$^2$, ranging between 0.01 and 1.14 mm$^2$.

A statistically significant longitudinal change in the area within the hyperautofluorescent ring was observed (*P* < .001). The analysis of FAF parameters is summarized in Table 3. A representative case is presented in Figure 2.

• OCT ANALYSIS: Table 3 summarizes the longitudinal assessment of OCT parameters. Central macular thickness (CMT) ranged between 151 and 726 μm at baseline, with a mean of 286.9 ± 101.8 μm. At follow-up, the mean CMT
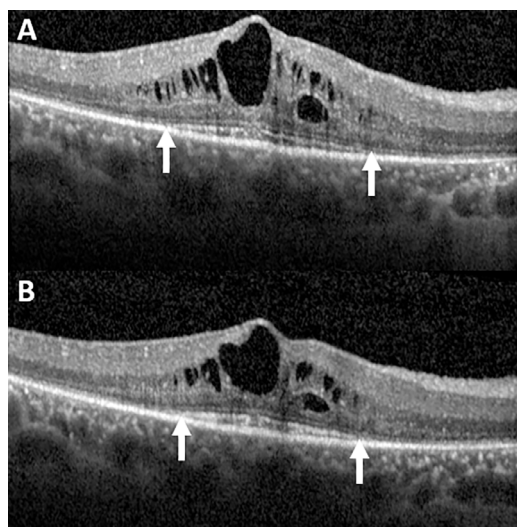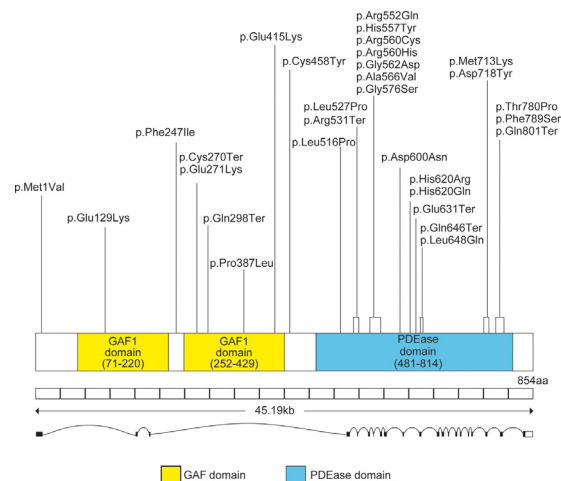
FIGURE 3. Optical coherence tomography (OCT) of a 43-year-old patient with *PDE6B*-associated retinitis pigmentosa. The reduction of the horizontal ellipsoid zone width (EZW) over 2 years is shown. The white arrows mark the border of the EZW at baseline (A) and at follow-up (B). The patient had persistent cystoid macular edema (CMO) which was treated with topical dorzolamide 2% eye drops 3 times daily, with fluctuation over time but minimal treatment response.



FIGURE 4. A schematic diagram of the genetic and protein structures of PDE6B. The positions of detected *PDE6B* variants, excluding splice site alterations (outside of coding region) and frameshift variants which yield truncations, are illustrated (*PDE6B*: ID P35913; Uniprot; accessed January 2023). GAF domain = cGMP-specific phosphodiesterase; PDEAse = phosphodiesterase.

was 289.7 ± 128.7 μm (range 149-1013 μm). The higher CMT values were associated with patients who had CMO. Macular volume ranged from 5.15 to 10.77 mm$^3$ at baseline and from 5.15 to 15.05 mm$^3$ at last follow-up. The mean macular volume was 7.54 ± 1.04 mm$^3$ at baseline and 7.57 ± 1.55 mm$^3$ at follow-up. No significant differences were observed between the 2 visits for central macular thickness ($P = .286$) and macular volume ($P = .875$). The baseline macular volume data are plotted against age in Figure 1, B.

Horizontal EZW was evaluated in 65% of eyes, with a mean width of 1946.1 ± 917.2 μm (range 466-4016 μm) at baseline, and in 58.8% of eyes at follow-up, with a mean EZW of 1763.9 ± 827.9 μm (range 410-3435 μm). The reduction in EZW was statistically significant ($P \leq .001$), indicating progressive degeneration over time.

Forty-four eyes were diagnosed with CMO at baseline (55%), and 41 eyes had CMO at follow-up (51.3%). All eyes with CMO were treated empirically with topical carbonic anhydrase inhibitors (dorzolamide and/or brinzolamide) for at least 1 month, and up to 1 year. One patient received an intravitreal dexamethasone implant. Eighteen eyes out of 44 experienced variable reduction of CMO with treatment, and 14 had improvement in vision that ranged from 0.12 to 0.52 LogMAR. Representative OCT images are presented in Figure 3.

• MOLECULAR GENETICS: In total, 43 variants were identified in *PDE6B*, including 23 missense, 7 nonsense, 7 splice site alterations, 5 frameshift, and 1 initiator codon variant (Supplemental Table 1). Twenty-seven variants were previously reported, and 16 variants were novel. The identified variants are presented in Figure 4. The evolutionary conservation is presented in Supplemental Figure 1.

There were 21 pathogenic, 7 likely pathogenic, and 15 variants with uncertain significance (VUS). Sixteen patients were homozygous for the identified variants. Only 3 patients had 2 VUS (Patient 29, 35, and 37), 8 patients had a VUS and a second likely pathogenic or pathogenic variants. The most prevalent variants were c.2193+1G>A (8/80 alleles), c.1107+3A>G (5/80 alleles), c.1923_1969delinsTCTGGG, p.(Asn643AspfsTer29) (3/80 alleles), c.1860del, p.(His620GlnfsTer23) (3/80 alleles), c.1485dup, p.(Pro496AlafsTer5) (3/80 alleles), c.1580T>C, p.(Leu527Pro) (3/80 alleles), c.304C>A, p.Arg102Ser (3/80 alleles), and c.769C>T, p.Arg257Ter (3/80 alleles).

• GENOTYPE-PHENOTYPE ANALYSES: Eighteen patients were classified into genotype A (multiple null variants), 7 in genotype B (1 null and 1 non-null variants), and 15 in genotype C (multiple non-null variants). Statistically significant differences were identified in terms of the reduction of hyperautofluorescent ring area and the reduction of EZW.

Group A and C comparison showed a statistically significant difference for macular thickness and hyperautofluorescent ring area, with group C having more advanced disease. There was a statistically significant difference between group A and C and between group B and C in terms of EZW reduction, with Group C having more advanced disease.

| | Baseline | Follow-Up | Test of Sig. | P |
|---|---|---|---|---|
| **TABLE 3.** Longitudinal Assessment of Visual Acuity and Imaging Parameters | | | | |
| **Macular thickness (um)** | **(n = 79)** | **(n = 75)** | | |
| Min.-Max. | 151-726 | 149-1013 | Z = 1.067 | .286 |
| Mean ± SD. | 286.9 ± 101.8 | 289.7 ± 128.7 | | |
| Median (IQR) | 263 (256-368) | 256 (234.5-357.5) | | |
| **Macular Volume (mm$^3$)** | **(n = 76)** | **(n = 71)** | | |
| Min.-Max. | 5.15-10.77 | 5.15-15.05 | t = 0.158 | .875 |
| Mean ± SD. | 7.54 ± 1.04 | 7.57 ± 1.55 | | |
| Median (IQR) | 7.37 (6.92-7.94) | 7.41 (6.82-7.78) | | |
| **Hyperautofluorescent ring Area (mm$^2$)** | **(n = 80)** | **(n = 80)** | | |
| Not available | 9 (11.3%) | 10 (12.5%) | MH = 0.500 | 0.467 |
| No | 23 (28.8%) | 24 (30%) | | |
| Yes | 48 (60%) | 46 (57.5%) | | |
| | **(n = 34)** | **(n = 29)** | | |
| Min.-Max. | 1.59-21.14 | 1.38-16.55 | Z = 4.373[a] | <.001[a] |
| Mean ± SD. | 7.11 ± 4.13 | 6.13 ± 3.62 | | |
| Median (IQR) | 6.38 (4.76-8.15) | 6.01 (3.59-7.1) | | |
| **CMO** | **(n = 80)** | **(n = 80)** | | |
| NA | 1 (1.3%) | 3 (3.8%) | MH = 2.500 | .096 |
| No | 35 (43.8%) | 36 (45%) | | |
| Yes | 44 (55%) | 41 (51.3%) | | |
| **EZW** Quatification | **(n = 80)** | **(n = 80)** | | |
| NA | 17 (21.3%) | 18 (22.5%) | MH = 2.000 | .109 |
| No | 11 (13.8%) | 15 (18.8%) | | |
| Yes | 52 (65.0%) | 47 (58.8%) | | |
| **EZW (um)** | **(n = 52)** | **(n = 47)** | | |
| Min.-Max. | 466-4016 | 410-3435 | Z = 5.539[a] | <.001[a] |
| Mean ± SD. | 1946.1 ± 917.2 | 1763.9 ± 827.9 | | |
| Median (IQR) | 1921 (1264.5-2732) | 1832 (1050.5-2405.5) | | |
| **BCVA (LogMAR)** | **(n = 80)** | **(n = 76)** | | |
| Min.-Max. | −0.12-2.80 | 0.0-2.80 | Z = 2.303[a] | .021[a] |
| Mean ± SD. | 0.56 ± 0.72 | 0.63 ± 0.73 | | |
| Median (IQR) | 0.30 (0.18-0.44) | 0.30 (0.18-0.48) | | |

BCVA = best corrected visual acuity; CMO = cystoid macular edema; EZW = ellipsoid zone width; IQR = interquartile range; n = eyes.

t: Paired t-test, Z: Wilcoxon signed ranks test, MH: marginal homogeneity test.

P: P value for comparing between baseline and Follow-up.

[a]Statistically significant at P ≤ .05; Sig. = significance.

Patients in group C had a mean age of 11 years greater than patients in Group A. Parameters and age for each group are presented in Table 4.

## DISCUSSION

This study presents a comprehensive analysis of the clinical and genetic characteristics of 80 eyes of 40 patients with molecularly confirmed PDE6B-related retinopathy, encompassing cross-sectional and longitudinal aspects. This represents one of the largest cohorts to date, allowing for indepth investigation through multimodal retinal imaging and genotype-phenotype assessment. The results offer insights into the retinal phenotype and natural history across a wide age range and identify 16 novel sequence variants.

All participants had a confirmed diagnosis of RP caused by sequence variants in PDE6B. The average age of diagnosis was 17.9 years, with an average age of symptom onset at 6.9 years, indicating that the disease often manifests during childhood. Nyctalopia was the primary presenting symptom, observed alone in 67.5% of patients at onset, with the remaining cohort presenting with peripheral visual field constriction. One patient was asymptomatic at diagnosis but was identified through the diagnosis of a symptomatic sibling. Visual acuity was assessed at baseline and follow-up. At baseline, 17.5% of eyes exhibited no visual

**TABLE 4.** Comparison Between the 3 Groups According to Different Parameters at Baseline (Mean ± SD)

| Parameter | Group A | Group B | Group C | Statistical Significance |
|---|---|---|---|---|
| Macular thickness (um) | 313.7 ± 120.3 | 291.8 ± 63.58 | 255.7 ± 83.31 | $P_1$ = .883, **$P_2$ = .018**[a], $P_3$ = .064 |
| Macular volume (mm³) | 7.79 ± 1.16 | 7.17 ± 0.92 | 7.38 ± 0.93 | $P_1$ = .062, **$P_2$ = .014**[a], $P_3$ = .996 |
| Ring Area (mm²) | 8.42 ± 4.25 | 5.59 ± 2.42 | 3.95 ± 1.45 | $P_1$ = .218, **$P_2$ = .002**[a], $P_3$ = .185 |
| Ellipsoid Zone Width (um) | 1920.4 ± 891.6 | 2073.9 ± 591.8 | 1326.4 ± 604.7 | $P_1$ = .473, **$P_2$ = .018**[a], **$P_3$ = .013**[a] |
| Age (year) | 38.44 ± 17.86 | 34.17 ± 13.35 | 49.38 ± 20.72 | $P$ = .134 |

$P$1: $P$ value for comparing between Groups A and B.
$P$2: $P$ value for comparing between Groups A and C.
$P$3: $P$ value for comparing between Groups B and C.
[a]Statistically significant at $P \leq$ .05.

impairment, while the remaining eyes showed varying degrees of visual acuity impairment, ranging from mild to severe. The majority (56.2%) had mild visual impairment. The follow-up period ranged from 0.25 to 12 years, and while there were variations in visual acuity over time, there was no statistically significant overall change. The BCVA mean at baseline was 0.56 ± 0.72 LogMAR, while at follow-up, it was 0.63 ± 0.73. This value is worse than the mean BCVA documented in Kuehlewein et al[19] (24 patients) and Khateb et al[20] (35 patients) studies (0.3 LogMAR and 0.4 LogMAR, respectively). The mean age of our subjects was 42.1 ± 19.0 years, compared to a mean age of 32.1 and 41.6 years in the other 2 studies, respectively. CMO was present in more than 50% of our cohort (compared to 30% in both other cohorts).

FAF analysis was available for most eyes and revealed a parafoveal hyperautofluorescent ring, a common finding in RP.[21] The inner border of the ring delineates the limits of a relatively intact ellipsoid zone on OCT.[22,23] The ring was present in the majority of eyes at both visits, its area decreased over time, coinciding with observed EZ loss on OCT. Vitor et al[24] also described a reduction of this hyperautofluorescent ring in their study of seven patients with PDE6A or PDE6B-related RP, with a rate of reduction of 0.32 ± 0.18 mm² per year. This ring is an important finding in patients with RP as it correlates with visual function.[21] Retinal sensitivity has been found to be relatively well preserved within the ring and conversely low or absent in retinal locations outside the ring.[23,25-27]

We report a slow reduction in the EZW over time, which reflects the slowly progressive degenerative process in PDE6B-related RP. In the Khateb et al[20] study, the retrospective data of 35 PDE6B-associated RP patients of 26 families were reviewed, while in Kuehlewein et al[19], 48 eyes were reviewed of which 44 eyes had OCT data available. The mean baseline EZW was comparable in all 3 studies. Longitudinal analysis of EZW was reported by Khateb et al[20], and a statistically significant difference was found between the rate of change of horizontal against vertical diameters of the preserved EZ. The annual loss of horizon-

tal EZW was −81.49 μm and was similar to our cohort, −99.81 μm. OCT analysis provided further insights into macular characteristics. Despite the presence of CMO in a significant number of eyes, there was no significant change in CMT or macular volume over time, suggesting relative stability in these parameters. It is possible that progressive thinning due to degeneration is masked by macular thickening due to CMO.

Forty-three PDE6B variants, including 16 novel variants were detected in the current large cohort study. The proportion of missense variants (23/43, 53.5%), splice site alterations (7/43, 16.3%), and truncating or initiator codon variants (13/43, 30.2%) observed in this cohort was compatible to those of the other large cohort study previously reported by Khateb et al[20] (missense 15/28, 53.6.4%; splice site alteration 4/28, 14.3%; truncating 9/28, 32.1%). These findings imply various types of variants spanning the entire protein cause disease in PDE6B-related retinopathy. Sixteen novel variants were identified, namely 7 missense variants (7/16, 43.8%), 5 splice site alterations (5/16, 31.3%), 3 stop variants (3/16, 18.8%), and 1 frameshift (1/16, 6.3%). Nine of these were classified into pathogenic (9/16, 56.3%) and all 7 missense variants were classified as VUS. Further data including segregation, as well as experimental investigations, could help clarify the pathogenicity of newly discovered missense variants. We identified a genotype-phenotype association, which may have been influenced by the age difference between the different genotypic groups. Statistically significant results were identified in both the reduction of hyperautofluorescent ring area and the reduction of EZW. Group A and C comparison showed a statistically significant difference for macular thickness and hyperautofluorescent ring area, which reflects that group C had more advanced disease. There was a statistically significant difference between Groups A and C and between Groups B and C in terms of EZW reduction, with Group C having more advanced disease, contrary to what would generally be expected. Patients in Group C had a mean age of 11 years greater than patients in Group A. The distribution of age in our cohort was as follows; most of both Groups A and B

patients were younger than 45 years, while in Group C, the majority were older than 45 years. In Group A ($n = 18$), we had 3 children, 3 teens, 8 patients between 24 and 45 years, and 5 patients above 45 years of age. Group B ($n = 6$) were all younger than 45 years except 1 patient. In Group C ($n = 16$), all patients were older than 45 except 5 patients. This age distribution and variable interval time between baseline and follow-up for each patient may have affected our findings. Furthermore, genotype-phenotype correlations may be difficult to be established; and in some cases not relevant for the disease course. A larger sample size would be necessary for further extrapolation of these findings.

The mean age of onset of nyctalopia, which was the presenting symptom in all groups, was $5.2 \pm 2.6$ for Group A, $9.4 \pm 2.3$ for Group B, and $6.8 \pm 3.9$ for Group C. Although the onset of nyctalopia was during early years of age in all groups, the onset of reduced BCVA was earlier in Group A and most delayed in Group B. The mean age of reduced BCVA in Group A was $12.0 \pm 7.5$ years, and Group B was $10.3 \pm 2.0$ years, while Group C was the last to show visual acuity decline and the mean age was $21.8 \pm 14.0$ years. The small number of each group has made the distribution of age an important factor influencing results.

• LIMITATIONS: Limitations of the study include its retrospective design, varying follow-up intervals and devices used, and the presence of CMO in over half of the cohort could also affect EZW measurements. While this study included the largest population with genetic results, larger samples are necessary to fully correlate structural and functional measures and assess progression rates. In the current study, patients with variants of uncertain significance were included based on the uniform presentation and the lack of other candidate genes.

• FUTURE DIRECTIONS: The promising findings of retrospective studies that highlight a wide therapeutic window, along with advances in molecular testing and high-resolution imaging, pave the way for prospective natural history studies and investigational clinical trials.[28] These studies are essential for investigating retinal function and structure,[29,30] prognosis, and phenotype-genotype correlations. Standardized protocols for timely assessments preceding interventional trials are crucial. Currently, a clinical trial on the safety and efficacy of gene therapy in human patients with RP caused by biallelic mutations in the *PDE6B* gene is ongoing (NCT03328130)[19]

• CONCLUSIONS: In summary, this study offers detailed insights into the clinical presentation of patients with *PDE6B*-related RP, encompassing age at onset, symptomatology, and functional and structural parameters such as visual acuity, hyperautofluorescent ring, macular thickness, volume, and EZW. The findings indicate relative stability in macular parameters despite the presence of CMO, with slow disease progression evidenced by a reduction in EZW, an essential anatomical endpoint. Most patients displayed no to mild visual impairment. These findings are expected to influence the design of future prospective natural history studies and interventional trials for *PDE6B*-related RP, as well as guide patient prognosis.

---

# CREDIT AUTHORSHIP CONTRIBUTION STATEMENT

**Shaima Awadh Hashem:** Writing – review & editing, Writing – original draft, Data curation, Conceptualization. **Michalis Georgiou:** Writing – review & editing, Writing – original draft, Supervision, Resources, Methodology, Investigation, Data curation, Conceptualization. **Yu Fujinami-Yokokawa:** Writing – review & editing, Writing – original draft. **Yannik Laich:** Formal analysis, Data curation. **Malena Daich Varela:** Methodology, Investigation, Formal analysis. **Thales A.C. de Guimaraes:** Writing – original draft, Validation, Conceptualization. **Naser Ali:** Writing – review & editing, Writing – original draft. **Omar A. Mahroo:** Writing – review & editing, Writing – original draft, Formal analysis. **Andrew R. Webster:** Writing – original draft, Data curation. **Kaoru Fujinami:** Writing – review & editing, Writing – original draft, Data curation. **Michel Michaelides:** Writing – review & editing, Writing – original draft, Supervision, Resources, Project administration, Methodology, Investigation, Funding acquisition, Formal analysis, Data curation.

---

# REFERENCES

1. Tee JJL, Smith AJ, Hardcastle AJ, Michaelides M. RPGR-associated retinopathy: clinical features, molecular genetics, animal models and therapeutic options. *Br J Ophthalmol.* 2016;100(8):1022–1027. doi:10.1136/BJOPHTHALMOL-2015-307698.

2. Rolling F, Le Meur G, Stieger K, et al. Gene therapeutic prospects in early onset of severe retinal dystrophy: restoration of vision in RPE65 Briard dogs using an AAV serotype 4 vector that specifically targets the retinal pigmented epithelium. *Bull Mem Acad R Med Belg.* 2006;161:10–12.

3. Hartong DT, Berson EL, Dryja TP. Retinitis pigmentosa. *Lancet.* 2006;368(9549):1795–1809. doi:10.1016/S0140-6736(06)69740-7.

4. Daiger SP, Bowne SJ, Sullivan LS. Perspective on genes and mutations causing retinitis pigmentosa. *Arch Ophthalmol.* 2007;125(2):151–158. doi:10.1001/ARCHOPHT.125.2.151.

5. Khramtsov NV, Feshchenko EA, Suslova VA, et al. The human rod photoreceptor cGMP phosphodiesterase $\beta$-subunit. Structural studies of its cDNA and gene. *FEBS Lett.* 1993;327(3):275–278. doi:10.1016/0014-5793(93)81003-I.

6. Kim MS, Joo K, Seong MW, et al. Genetic mutation profiles in Korean patients with inherited retinal diseases. *J Korean Med Sci.* 2019;34(21). doi:10.3346/JKMS.2019.34.E161.

7. Yeo JH, Jung BK, Lee H, et al. Development of a Pde6b gene knockout rat model for studies of degenerative retinal diseases. *Invest Ophthalmol Vis Sci.* 2019;60(5):1519–1526. doi:10.1167/IOVS.18-25556.

8. Cote RH. Characteristics of photoreceptor PDE (PDE6): similarities and differences to PDE5. *Int J Impot Res.* 2004;16(1):S28–S33. doi:10.1038/SJ.IJIR.3901212.

9. Mahato B, Kaya KD, Fan Y, et al. Pharmacologic fibroblast reprogramming into photoreceptors restores vision. *Nature.* 2020;581(7806):83–88. doi:10.1038/S41586-020-2201-4.

10. Bennett J, Tanabe T, Sun D, et al. Photoreceptor cell rescue in retinal degeneration (rd) mice by in vivo gene therapy. *Nat Med.* 1996;2(6):649–654. doi:10.1038/NM0696-649.

11. Pang JJ, Lei L, Dai X, et al. AAV-mediated gene therapy in mouse models of recessive retinal degeneration. *Curr Mol Med.* 2012;12(3):316–330. doi:10.2174/156652412799218877.

12. Pichard V, Provost N, Mendes-Madeira A, et al. AAV-mediated gene therapy halts retinal degeneration in PDE6$\beta$-deficient dogs. *Mol Ther.* 2016;24(5):867–876. doi:10.1038/MT.2016.37.

13. SparingVision's lead asset SPVN06 clears IND application in US for treatment of retinitis pigmentosa. Accessed January 19, 2024. https://www.ophthalmologytimes.com/view/sparingvision-s-lead-asset-spvn06-clears-ind-application-in-us-for-treatment-of-retinitis-pigmentosa

14. Georgiou M, Robson AG, Jovanovic K, et al. RP2-associated X-linked retinopathy: clinical findings, molecular genetics, and natural history. *Ophthalmology.* 2023;130(4):413–422. doi:10.1016/J.OPHTHA.2022.11.015/ATTACHMENT/1CCF9AE8-B9E9-4A80-99E4-1E921B34DFCB/MMC6.PDF.

15. Lange C, Feltgen N, Junker B, Schulze-Bonsel K, Bach M. Resolving the clinical acuity categories "hand motion" and "counting fingers" using the Freiburg Visual Acu-

16. Lefter M, Vis JK, Vermaat M, den Dunnen JT, Taschner PEM, Laros JFJ. Mutalyzer 2: next generation HGVS nomenclature checker. *Bioinformatics.* 2021;37(18):2811. doi:10.1093/BIOINFORMATICS/BTAB051.

17. Richards S, Aziz N, Bale S, et al. Standards and guidelines for the interpretation of sequence variants: a joint consensus recommendation of the American College of Medical Genetics and Genomics and the Association for Molecular Pathology. *Genet Med.* 2015;17(5):405–424. doi:10.1038/GIM.2015.30/ATTACHMENT/7A004D0E-5CC1-4A04-8892-2F9B13D8ACB7/MMC1.PDF.

18. Abou Tayoun AN, Pesaran T, DiStefano MT, et al. Recommendations for interpreting the loss of function PVS1 ACMG/AMP variant criterion. *Hum Mutat.* 2018;39(11):1517–1524. doi:10.1002/HUMU.23626.

19. Kuehlewein L, Zobor D, Stingl K, et al. Clinical phenotype of pde6b-associated retinitis pigmentosa. *Int J Mol Sci.* 2021;22(5):1–15. doi:10.3390/ijms22052374.

20. Khateb S, Nassisi M, Bujakowska KM, et al. Longitudinal clinical follow-up and genetic spectrum of patients with rod-cone dystrophy associated with mutations in PDE6A and PDE6B. *JAMA Ophthalmol.* 2019;137(6):669–679. doi:10.1001/jamaophthalmol.2018.6367.

21. Tee JJL, Kalitzeos A, Webster AR, Peto T, Michaelides M. Quantitative analysis of hyperautofluorescent rings to characterize the natural history and progression in RPGR-associated retinopathy. *Retina.* 2018;38(12):2401–2414. doi:10.1097/IAE.0000000000001871.

22. Aizawa S, Mitamura Y, Hagiwara A, Sugawara T, Yamamoto S. Changes of fundus autofluorescence, photoreceptor inner and outer segment junction line, and visual function in patients with retinitis pigmentosa. *Clin Exp Ophthalmol.* 2010;38(6):597–604. doi:10.1111/J.1442-9071.2010.02321.X.

23. Fakin A, Jarc-Vidmar M, Glavač D, Bonnet C, Petit C, Hawlina M. Fundus autofluorescence and optical coherence tomography in relation to visual function in Usher syndrome type 1 and 2. *Vision Res.* 2012;75:60–70. doi:10.1016/J.VISRES.2012.08.017.

24. Takahashi VKL, Takiuti JT, Jauregui R, Lima LH, Tsang SH. Structural disease progression in PDE6-associated autosomal recessive retinitis pigmentosa. *Ophthalmic Genet.* 2018;39(5):610–614. doi:10.1080/13816810.2018.1509354.

25. Popović P, Jarc-Vidmar M, Hawlina M. Abnormal fundus autofluorescence in relation to retinal function in patients with retinitis pigmentosa. *Graefes Arch Clin Exp Ophthalmol.* 2005;243(10):1018–1027. doi:10.1007/S00417-005-1186-X.

26. Lenassi E, Troeger E, Wilke R, Hawlina M. Correlation between macular morphology and sensitivity in patients with retinitis pigmentosa and hyperautofluorescent ring. *Invest Ophthalmol Vis Sci.* 2012;53(1):47–52. doi:10.1167/IOVS.11-8048.

27. Greenstein VC, Duncker T, Holopigian K, et al. Structural and functional changes associated with normal and abnormal fundus autofluorescence in patients with retinitis pigmentosa. *Retina.* 2012;32(2):349–357. doi:10.1097/IAE.0B013E31821DFC17.

28. Georgiou M, Kalitzeos A, Patterson EJ, Dubra A, Carroll J, Michaelides M. Adaptive optics imaging of inherited retinal diseases. *Br J Ophthalmol.* 2018;102(8):1028–1035. doi:10.1136/BJOPHTHALMOL-2017-311328.

29. Varela MD, Esener B, Hashem SA, De Guimaraes TAC, Georgiou M, Michaelides M. Structural evaluation in inherited retinal diseases. *Br J Ophthalmol.* 2021;105(12):1623–1631. doi:10.1136/bjophthalmol-2021-319228.

30. Daich Varela M, Georgiou M, Hashem SA, Weleber RG, Michaelides M. Functional evaluation in inherited retinal disease. *Br J Ophthalmol.* 2022;106(11):1479–1487. doi:10.1136/BJOPHTHALMOL-2021-319994.